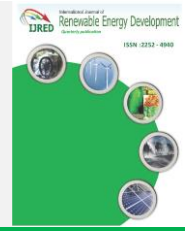




Contents list available at IJRED website

Int. Journal of Renewable Energy Development (IJRED)

Journal homepage: <https://ijred.undip.ac.id>



Research Article

Sustainable Design of a Near-Zero-Emissions Building Assisted by a Smart Hybrid Renewable Microgrid

Mostafa Esmaili Shayan¹, Gholamhassan Najafi^{1,*}, Barat Ghobadian¹, Shiva Gorjian¹, Mohamed Mazlan^{2**}.

¹Department of Mechanical and Biosystems Engineering, Tarbiat Modares University (TMU), Tehran, Iran.

²Advanced Material Research Cluster, Faculty of Bioengineering and Technology, University of Malaysia Kelantan, Jeli, Kelantan, Malaysia

Abstract. Renewable energy regulations place a premium on both the use of renewable energy sources and energy efficiency improvements. One of the growing milestones in building construction is the invention of green cottages. Building Integrated Photovoltaic (BIPV) technologies have been proved to aid buildings that partially meet their energy demand as sustainable solar energy generating technologies throughout the previous decade. Curved facades provide a challenge for typical photovoltaics. This study designed, produced, and assessed elastic solar panels supported by flexible photovoltaic systems (FPVS) on a 1 m² layer. The LabVIEW program recognizes and transmits online data on warm and dry climates. The fill factor was 88% and 84%, respectively, when installed on the silo and biogas surfaces. The annual energy output was 810 kWh on a flat surface, 960 kWh on a cylindrical surface, and 1000 kWh on a hemisphere surface. Economic analysis indicates that the NPV at Flat surface is \$ 697.52, with an IRR of 34.81% and an 8.5-year capital return period. Cylindrical surfaces and hemispheres both get a \$ 955.18 increase. For cylindrical and hemispheric buildings, the investment yield was 39.29% and 40.47%, respectively. A 20% increase in fixed investment boosted the IRR by 21.3% in the flat system. While the cylindrical system had a 25.59% raise, the hemisphere saw a 24.58% gain.

Keywords: Green Cottages; Building Integrated Photovoltaic; Sustainable; Flexible Photovoltaic Systems; LabVIEW

Article history: Received: 2nd Jan 2022; Revised: 8th February 2022; Accepted: 15th February 2022; Available online: 25th February 2022

How to cite this article: Esmaili Shayan, M., Najafi, G., Ghobadian, B., Mazlan, M. (2022) Sustainable Design of a Near-Zero-Emissions Building Assisted by a Smart Hybrid Renewable Microgrid. *International Journal of Renewable Energy Development*, 11(2), 471-480 <https://doi.org/10.14710/ijred.2022.43838>

1. Introduction

The Kyoto Protocol is an international agreement related to the UN on climate change, which requires countries worldwide to set specific carbon reduction targets around the world. The main concern of environmental policymakers is climate change mitigation. The impact of various factors on GHG emissions has been studied by many authors (Liobikienė *et al.*, 2021). Despite supply chain issues and construction delays caused by the pandemic, renewable capacity additions in 2020 increased by over 45% from 2019. Global wind capacity additions increased by 90%. Also underpinning this record growth was the 23% expansion of new solar PV installations to almost 135 GW in 2020 (Jäger-Waldau, 2021). Utility-scale applications will account for about 70% of annual PV additions by 2022, up from 55% in 2020. Although China's significant FITs for commercial and industrial PV projects increased the ratio of distributed projects from 25% in 2016 to nearly 45% in 2018, this trend reversed in 2019 (IEA, 2021). In the last decades, photovoltaic (PV) technology has been drawing enormous attention worldwide. In the future, solar energy consumption is expected to increase

due to further reductions in prices in solar cell technology (Braito *et al.*, 2017; Hasanien, 2018). Aside from the non-linear nature and environmental dependability of PV systems, the conversion of energy by PV panels is undesirable (Skordoulis *et al.*, 2020). It is a positive step towards obtaining energy from light through the advancement of science. Thanks to further cost reductions and continuous policy support from 120 governments globally, PV capacity additions are forecast to expand to 162 GW in 2022 (O'Shaughnessy *et al.*, 2021; Tsantopoulos *et al.*, 2014). Despite the ongoing COVID-19 pandemic, the overall investments in solar energy increased by 12% to USD 148.6 billion (EUR 125 billion). In 2020, over 135 GW of new solar photovoltaic electricity generation capacity was installed increasing the total cumulative installed capacity to over 770 GW (Jäger-Waldau, 2021). The quality of electricity and the various sources of supply are now seen as the core solutions of policymakers around the world. Fossil fuels fall from almost four-fifths of total energy supply today to slightly over one-fifth (Najafi *et al.*, 2011). Some of the most challenging environmental problems are the production and usage of oil resources and greenhouse gases. Every year, non-renewable energy

* Correspondence author: g.najafi@modares.ac.ir / ** mazlan.m@umk.edu.my

releases a megatonne of greenhouse gases (GHG) into the atmosphere (Awad *et al.*, 2017; Muhammad-Sukki *et al.*, 2011). In South Asia, the concept of using skin-based solar systems is on the increase. BIPV is increasingly used as a primary or secondary energy source in buildings. Unique criteria for the proper efficiency of the BIPV cells need to be regarded. Building-integrated photovoltaics (BIPV) is one of the most promising contributors to net-zero energy buildings, while also increasing the aesthetic value of the built environment and Thermal and sound insulation properties (Briguglio *et al.*, 2017). The electrical power from the solar cells is increased by reducing the operating temperature. Like all other semiconductor devices, solar cells are sensitive to temperature. Temperature increases reduce the bandgap of a semiconductor which leads to the decrease of the module efficiency and output power (Mohsen Azadbakht *et al.*, 2015; Zeb *et al.*, 2014). Using natural or forced ventilation systems is one of the most effective ways to lower the solar cell temperature and reduce efficiency. In addition, the solar system designer can position the solar cell in the direction of the wind at the correct position (Rabab Mudakkar *et al.*, 2013; Shukla *et al.*, 2018). Iran's energy intensity index is up by a factor of 3. Developing countries can be expected to find themselves in a similar position. For developed countries, this index is about 0.3 (Esmaeili Shayan, *et al.*, 2021; Etefaghi *et al.*, 2018). An increasing human population and the need for energy usage, limitations and inability to react to refined petroleum products have increased the desire to use renewable energy, especially solar energy. Regardless of this, electricity demand per household has increased dramatically over 2007-2018 (Al-Falahi *et al.*, 2019). It is expected that this growth will occur until 2030 and that the slope will reach 60 percent (Azadbakht *et al.*, 2015). In the supply of renewable energy and considered Iran's capacity, solar energy is environmentally sustainable, leading to non-CO₂ generation; it also contributes to natural resource sustainability, land recovery, reduced power transmission lines, increased regional energy control, improved speed and cost-effectiveness of electricity transmission into rural areas (Solangi *et al.*, 2011). Iran's Central Bank has reported that this sector's inflation rate was 10 percent a year based on the average inflation rate between 2011 and 2016 (Salehi-Isfahani *et al.*, 2018). Research surveys have estimated that Tehran's sunny days and hours are about 313 days and 1742 hours a year, respectively. The increase from the southeast to the northwest of Iran is reduced, whereas it usually increases from the west to the east (Esmaeili Shayan, 2020). The irradiance map and statistical irradiance simulations show that irradiance level in clear air is theoretically high in Iran, including Yazd, Kerman, Tabas, Birjand, Iranshahr, Chabahar, Shiraz, Bam, Bushehr, and desert areas. However, building construction does not usually permit traditional solar systems with rigid modules (Esmaeili shayan *et al.*, 2020). The flexible solar cells can generate voltages of more than 50V. These circuits will contain appliances voltage requiring higher setup power in normal mode (Mohsen Azadbakht *et al.*, 2013; Chen *et al.*, 2019). Major market trends are described as the inverter, module size, main power, and deployment and Balance of System (BOS) cost decline. With a cumulative annual growth rate of 200th Compound (CAGR), the cost of modules is forecast to decline from 260 cents/Wp in 2009 to 30 cents/Wp in 2018

(Padmanathan *et al.*, 2018). The building's shape directly affects its energy use. Modern architecture regularly uses curved forms. They have a significant impact on the building's solar and energy performance, and may improve the internal environment. The curved shape is also used on silos, biogas tanks, greenhouses and structures. The Taguchi factorial experiment and response surface methods are used to improve the precision of the test and reduce the expense of testing and speed up the experiment (Dehghan *et al.*, 2021). Conventional solar panels involve the construction of glass panels that are usually not quite consistent with cylindrical geometric shapes (Keshtegar *et al.*, 2018). One of the solutions to these problems is the development and production of solar systems focused on flexible panels that, in addition to supporting the architecture of the desired structures and sustaining the previous capabilities, are economical and provide the energy needs of the electrical equipment for these structures (Ghritlahre *et al.*, 2018). Rural electrification in Iran was started by using photovoltaics in 2006 (Esmaeili Shayan *et al.*, 2020; Najafi *et al.*, 2007). Hydrocarbons dominate Iran's energy mix. Traditional thermal power plants run on natural gas and petroleum derivatives such as gasoline and fuel oil. The remaining 2% comes from hydropower, nuclear, biofuels, and other renewables (Mat Yasin *et al.*, 2017). Solar power plants have the least capacity of the three grid-connected power plants (wind, biogas, and solar) mounted. Wind provides the majority of renewable energy capacity [29,30].

The popularity of photovoltaic technology has expanded over the previous decade due to the good consequences, the convenience of investing in photovoltaics, and the performance of photovoltaics. The research addressed a knowledge gap on the desire of certain older and historic buildings to invest in photovoltaics. Additionally, the study findings enabled greater understanding of the elements that influence investment decisions in photovoltaics. Flexible Photovoltaic Systems are suitable for buildings with complex shape envelopes, such as harvest silos, traditional Islamic buildings, and Petrochemical Tanks. This critical phase can provide a portion of the electrical energy while preserving geometric and aerodynamic properties. This study explores the potential of a flexible solar conversion device for energy supply on curved surfaces. In this research, we used environmental assessment, and environmental approaches focused on pilot projects to use the actual capacity of a flexible solar energy conversion system.

2. Materials and Methods

Flexible layers with suitable depth and durability can cover any design and introduce more incredible energy with selected columns. Fig.1 illustrates the system's hardware schematic and a block diagram of the voltage control system and FPV power plant's components. The components involved in the solar energy system were modeled in flat, cylindrical, and hemispherical shapes and studied under actual conditions. Data from irradiance, temperature, humidity, wind speed were recorded every 30 minutes through the data logger and sent to LabVIEW software via USB-4711A device. A power meter measures and records the voltage, current, and output power of the systems. Throughout this process, the test layer was

placed at 1 m², and the analysis and design of the radial and axial shapes were taken out

The Solar power conversion model based on flexible panels, as shown in Fig. 2 includes: geometric arrangement on cylindrical, hemispheric and flat surfaces, flexible solar cell, battery block, irradiance meter, temperature sensor, humidity sensor, anemometer, voltage monitor, power amplifier, planning circuits, battery plugs and fuses, analog-digital converter. Moreover, the Ambient temperature and surface temperature of solar cells were measured using 16 complete circuits of lm35 sensor connected to USB4711A with 0.1 °C accuracy and an Extech AN200 Wind sensor with ± 5% accuracy in the wind speed range of 0.4 to 30 m/s.

The amorphous silicon (a-Si) element JNsolar3W-12v with three deposition junction points in a stainless polymer sheet and a lock diode has been used to resist the leakage of the battery current to the solar module panel (Bloem et al., 2012). The most efficient matching layer provided by choice of 1 m² solar panels could be 9744 cm². After removing the edges of the flexible solar panel, the photovoltaic section will be equal to 6996 cm². To cover the cylindrical and hemispherical surfaces with a specified area, 16 flexible solar elements, a cylindrical and hemispherical structure with a particular area is required. The structural models were created in SketchUp and the thermal stress analysis in Ansys Workbench showed a maximum strain of 0.041 mm in the radius direction. The strain was negligible, but to avoid rupturing the flexible parts, the contact distance was set at 2 mm. The RS232 device and the LabVIEW software package were used to attach the temperature module. The Fill factor (FF) is a parameter that, in conjunction with Voc and Isc, determines the maximum power from a solar cell. The FF is defined as the ratio of the maximum power from the solar cell to the product of Voc and Isc. The matching principle is quantitatively similar to the current-voltage supply series, and the higher the amount, the greater the photovoltaic system's output. The fill factor is calculated on the surface according to equation (1) (Abdolbaqi et al., 2016; Yan et al., 2015). The efficiency of a photovoltaic system is also one of the most critical external

measurement items. Efficiency (η) is defined by Equation (2) (Ghasemzadeh et al., 2020).

$$FF = \frac{V_{MPP} \times I_{MPP}}{V_{oc} \times I_{sc}} \tag{1}$$

$$\eta = \frac{P/S_t}{G} \tag{2}$$

Where G equals the irradiance (W/m²), St equals the array layer (m²), and P equals the device power at the target point (W). Use that indexing relationship to measure the output power in shadow mode, temperature shifts, dust fall, light reflection and solar activity on the solar array. Excel 2019 and Design Expert 7 and Minitab 18 were included. The optimal power system was validated using the Taguchi and Response Surface Methodology (RSM). Flexible solar panels are connected in series and off-grid from the mains with battery backup. Climatic data for the 27-day test was collected from the Meteorological Station and direct measurement instruments linked to the LabVIEW program. Table (1) shows the test factors and surfaces in the Taguchi and RSM designs. For this test, 4 variables were chosen: irradiance power at three levels, temperature, wind speed, and flexibility at 3 levels. The Taguchi test design and RSM method were analyzed based on maximum power generation capacity. Modeling in this test is evaluated based on the criterion "more power is better".

By analyzing the model's components, engineering economics will decide the rejection or acceptance of a project. COMFAR software has been used in this research, with the complexity of the system's economic variables and technological variables. The present value of costs is calculated analogously that of the benefits. The difference is that for this figure, the outflows are considered as representing costs, rather than the inflows. BCR is calculated by Equation (3).

$$BCR = \frac{|PV[Benefits]|}{|PV[Cost]|} \tag{3}$$

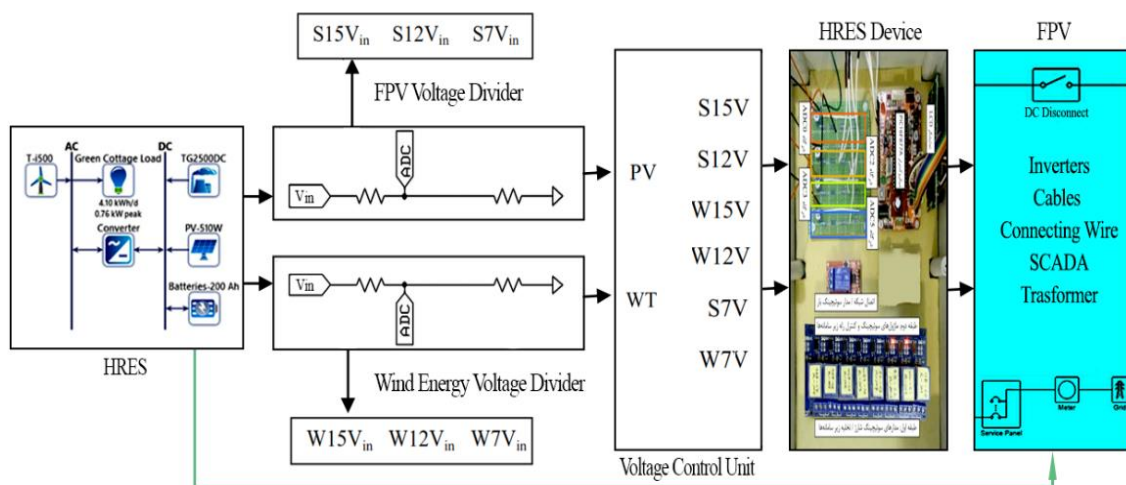


Fig.1 Hybrid renewable energy system components.

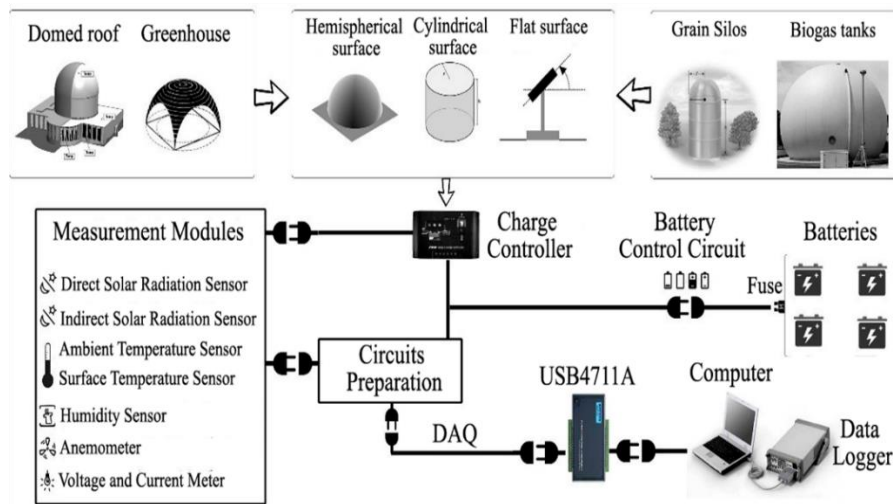


Fig.2 Flexible solar device and monitoring devices.

Table 1
 Levels and responses of Taguchi and RSM design.

Factor	Variables	Units	Taguchi			RSM	
			Level 1	Level 2	Level 3	Low Actual	High Actual
A	Irradiance	W/m ²	200-500	500-800	800-1100	200	1100
B	Temperature	°C	20-30	30-40	40-50	20	50
C	Wind Speed	m/s	0-1	1-2	2-3	0	3
D	Flexibility	Degree	Flat	Cylinder	Sphere	0	π

Table 2
 Green cottage electric consumers (Leonard et al., 2018).

Section	Consumption (W)	Current (A)	ON-Time (Hours)	Ampere Hourly (Ah)
Cooking	40-800	8.33	1	8.33
Entertainment	17-100	2.5	2	5
Lighting	5-10	2.28	5	11.45
Computer	50	4.16	8	33.28
Maintenance	20-100	3.33	24	79.9
Total	132-1060	20.6	-	137.96

Internal rate of return (IRR) is a well-known criterion in terms of projects' economic evaluation. The deposit interest rate in Iran has freshly reduced to 15%. However, in the last 10 years, it has equated to 16.7%, regarded as the benchmark discount rate. According to the Iranian parliament's legislation, each kilowatt of renewable electricity is purchased from the consumer at ~0.05 \$/kWh. This price is supposed to be 20 years of the solar system's useful lifetime (Esmaeili Shayan & Hojati, 2021). In (Esmaeili Shayan, Esmaeili Shayan, et al., 2021) the different feed-in tariff (FiT) rate is considered to be 0.05 \$/kWh. In addition, the project's NPV is set to zero and the discount rate, which is the same as the project's IRR, is determined. The calculation of the IRR is based on the NPV which can be expressed as a function of the IRR. Equation (4) uses cash flows at regular intervals for the calculation of IRR.

$$IRR = \frac{CF_i}{(1+r)^i} - C_{inv} \quad (4)$$

Where CF_i is cash flow in the period, r is the discount rate, i is time period and C_{inv} is initial investment. IRR calculate by COMFAR through trial and error because you are trying to arrive at whatever rate which makes the NPV equal to zero. The lifetime of the system is 20 years. The green cottage's electric customers are listed in Table (2).

3. Results and Discussion

JP solar 3W-12V flexible solar arrays generate flexible solar energy systems by fitting them to flat, cylindrical, and hemispheric base surfaces. The shape of I-V curve

changes with the change in Fill Factor of solar cell which has been shown in Fig. 3. The minimum values of FF were calculated as 0.73 for the flat surface and 0.88 and 0.84 for the cylindrical and hemispherical surfaces, respectively. When the radiation is at level one, the device will begin to operate. Irradiance ranges between 400 W/m² and 600 W/m²; then, the effectiveness is a little diminished, but it is still optimal for the system and satisfies the objective. More than 1000 W/m² of irradiance will have a negative impact on system performance. With an overall view of the irradiance power and the SNR band, it can be shown that irradiance intensity may substantially affect the function of the electrical power generation capacity through distancing itself from the center line and high failure.

The temperature in the latter group and the temperature level (3) had the most significant impact on the performance of the solar energy device. Incoming wind speed from level (1) to level (2) was useful for the subsystem and could change the conditions to produce power at extremely high temperatures. Flexibility or angles of the photovoltaic solar panels has shown that the change in this element, including the usage of the system in flat style (level 1) or when installed on a spherical surface (level 2) or on a cylindrical surface (level 3), may affect the production of the full power objective. The system angle group and the SNR revealed that level (1) defined as the flat surface layer might significantly affect the solar system. The application of the system at level (2), i.e. the application of the system to the spherical surface, considering its proximity to the middle power line goal, is

more efficient than the levels (1) and (3). Level (3) indicated that the application of the method to a cylindrical surface is more efficient than a flat surface, but the optimum output is at level (2). The use of the process on the roof in flat styles, such as bitumen, is therefore not taken priority. When a system needs both grain silos and biogas reservoirs in a farm simultaneously, the operation of the device under these conditions would be superior to the hemisphere level, which implies the biogas reservoir.

The largest effect on the function of the flexible photovoltaic system, is related to the rate of irradiance, wind speed, temperature, and use on various such as flat, cylindrical and spherical materials. In the present experiment, Taguchi's study found that if the device were evaluated at chosen levels based on the optimal manufacturing process and variables, it would be possible to predict a combined power of 49.9W with SNR = 33.929. If the function is measured separately and on a fully flat surface strength of the function, it would be equal to 53.3W with SNR = 34.4918. When the model was used to calculate the power on the cylindrical level, the device's power was equal to 54.05W with SNR = 34.6368; for the hemispheric level, the corresponding power of 55.7W with SNR = 34.8880 was measured. The choice of the hemispheric surface is then classified into first and second-level cylinder points. According to the Taguchi experiments, the dynamic conditions applied to the flexible solar system indicate the ideal conditions for the use of a flexible panel-based solar conversion system.

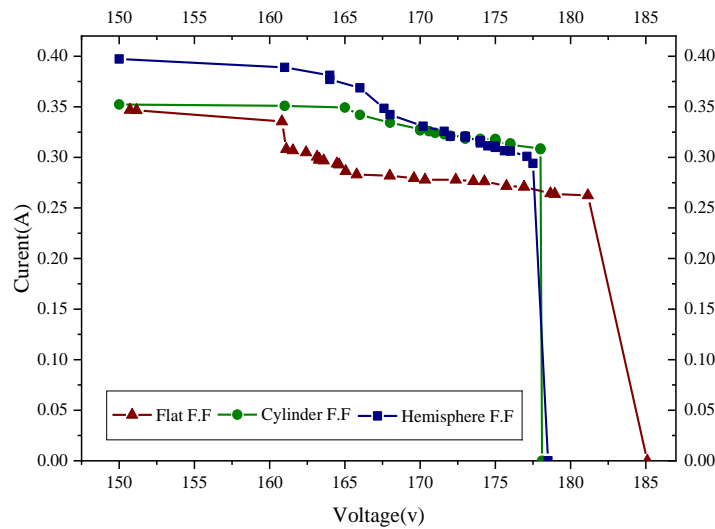


Fig 3. I-V Curve modification with varying FF.

Table 3
List of solar power production costs in systems at different surfaces.

Systems	Power Production (kWh.\$)	Total Revenue Per Year (\$)
Flat	810.369×0.05	40.518
Cylinder	960.124×0.05	48.006
Hemispherical	1000.165×0.05	50.008

The systems' production capacity is calculated over a period of a year. Performance-based flexible systems at their maximum power production conditions can have other revenues when deployed on different surfaces, according to Table 3. The flat surface system produced 810.369 kWh, the cylindrical surface 960.124 kWh, and the hemisphere surface 1000.165 kWh. Total Revenue Per Year can be calculated for each system if the feed-in tariff is set at \$0.05 Per kWh.

Therefore, 56 watts is equal to \$ 44.8 in 2020(Ghasemzadeh et al., 2020). Thin-film technology has always been cheaper but less efficient than conventional c-Si technology. However, it has significantly improved over

the years(Esmaeili Shayan *et al.*, 2020). The total cost of a flexible photovoltaic system including the purchase of panels, installation costs, etc. is estimated at \$ 181.78 according to the standard in current photovoltaic projects. Unforeseen costs included glue costs for reposing panels to surfaces, maintenance costs, and soil cleaning. The 20-year maintenance life of the solar system was estimated at \$ 20 per year. Sensitivity analysis is a calculation procedure that predicts the effects of changes on input data. Investment decisions are wracked with uncertainty and risk. As seen in Fig. 4, The irradiance peak is reached 1067.1 W/m².

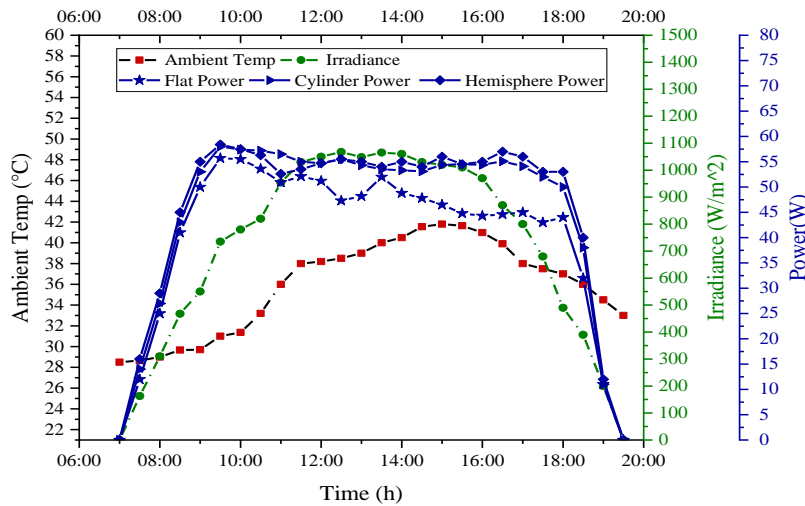
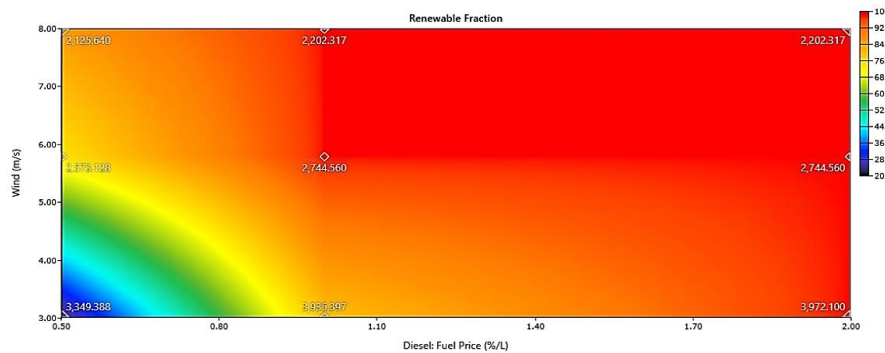
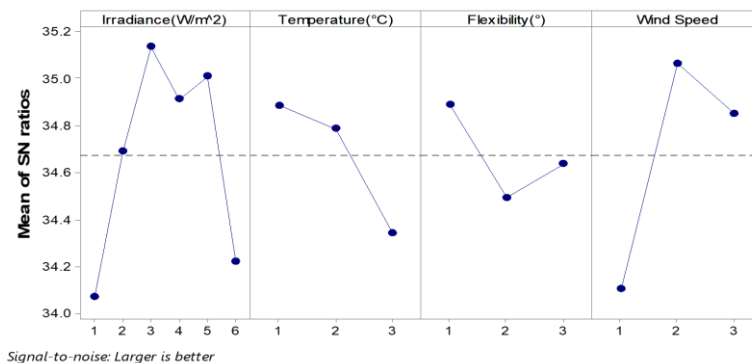


Fig 4. System factors and power analysis.



A: The system optimization



B: The Taguchi Signal-to-Noise ratio

Fig 5. The system optimization and effect of test variables in the real-time system modeling.

In the cylinder, one side of the shadow and one side of the irradiance are usually present. For at least 3 hours, the irradiance will be greater than 735 W/m². It is likewise at its peak in the middle of the day. At sunset, the irradiance will be at its lowest and will finally hit zero. After sunrise, the irradiance power on the south side of the test cylinder increased with a gentle slope, reaching a maximum of 1048 W/m² in the afternoon (around 14:00). These adjustments regulated the form of curved surfaces like the Sin Type. Power in the hemisphere increased after sunrise and reached a maximum of 58.4 W at the beginning of the day. At midday (from 09:30 to 17:30), the power potential was almost constant at the hemispherical and cylindrical surface and was within the standard line range (55.5 W). Then, as the shade increases and the intensity of the light falls, the power decreases to zero.

The maximum power in Taguchi Method Test is related to the system deployment on the cylinder facade and is equal to 59.87 W, while the minimum power of 57.84 W is related to the system when deployed on the flat surface, and maximum power in RSM Test is relevant to the system deployment on the hemispherical (H) surface and equal to 61.14 W and minimum power of system is 56.6 W when related to the extent on the flat surface. The system's performance (SP) under standard test conditions (STC) (25 °C and irradiance power of 1000 W/m²) and in the laboratory for deploying on the cylinder and hemispherical facades has been measured 7.45%. The minimum performance was measured at 7.09% and related to the flat surface. In the model analysis, the open-circuit voltage at the flat system level was equal to 185.7 volts and the short-circuit current reached 0.347 in the most optimum scenario. Furthermore, the maximum production current was 0.36 amps when the system was deployed on the hemispherical surface. Therefore, the system in the case of deployment on the hemispherical surface by receiving diffusion irradiances and vertical irradiances has optimal electrical and quality characteristics compared to other deployment surfaces. The second and third priorities are related to the cylindrical and flat surfaces, respectively.

This study has shown that using an experimental design of Taguchi and RSM can explain the big data of solar energy systems. When the actual test data in these models

will verify the correct orientation of the model. Fig.5 shows real-time system modeling. The system optimization revealed that by assuming an average wind speed of 3 m/s, eliminating the diesel generator, using three batteries, and increasing the capacity of the solar and wind subsystems, the cost of renewable energy production may be decreased to \$ 0.402 kWh.

The impact of test factors on system power is shown in Fig.5B. The irradiance and wind speed factors have a positive effect on the system power, whereas the temperature factor has a negative impact. the optimum power in the cylindrical surface is 60.27 watts, once the ambient temperature is about 36°C and radiation is 1050 W/m², and the wind speed is zero, and the humidity is equal to 48.1%. Sensitivity analysis is performed to predict the future. Fig.6 shows the sensitivity analysis of systems. The most sensitive parameters Sales revenue and on the flat surface and then Increase in fixed assets has a more significant impact on IRR. The investment attractiveness and IRR share of the flexible photovoltaic system are related to its use on flat, cylindrical, and hemisphere surfaces, respectively.

The economic findings show that the NPV of the flexible solar energy system at 16.70%, when applied at level 1, is \$ 697.52 and that the IRR is 34.81% and the capital return duration is 8.58 years. This amount is increased to \$ 900.88 in cylindrical surfaces and \$ 955.18 in hemispheres. The rate of return on investment was 39.29% at the cylindrical level and 40.47% at the hemisphere. In the flat-surface production method, a 20% rise in project budget raised the internal yield by 21.3% and a 20% fall in sales. The project's internal rate of return would be reduced by 23%. Flexible solar systems installed on cylindrical and hemispheric surfaces with a 20% rise in project prices, with the IRR rising by 25.59% and 24.48%, respectively. During the production time and deployment of flexible solar systems, the net flows were negative and when installed on cylindrical and hemispheric surfaces, from 7.20 years and 6.90 years to the end of the design period, the total net product flows were positive and constantly expanding. The description of the results is listed in Table 4.

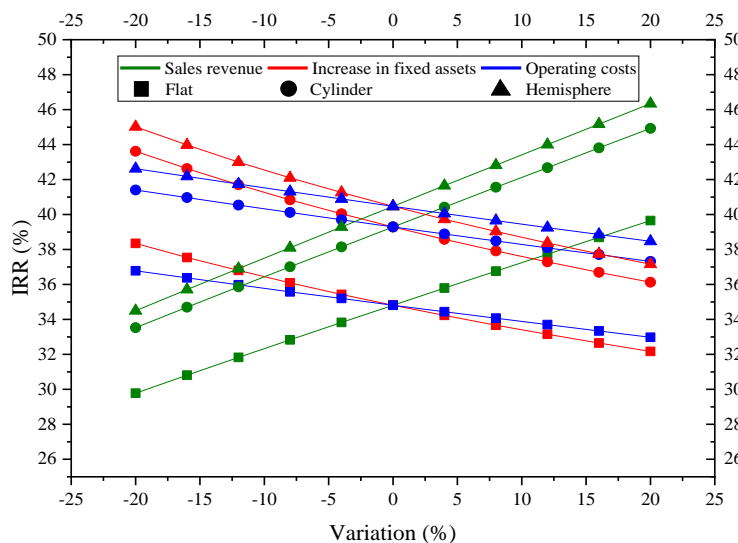


Fig 6. Effect of test variables on system power production quality in the actual test

Table 4
Systems behavioral assessment for more is great target

Power Plan	MP Taguchi (W)	MP RSM (W)	FF (%)	S.P (%)	OCV (V)	SCC (A)	IRR	NPV
Flat S.	57.84	56.6	73	7.1	185	0.34	34.8	697.5
Cylindrical S.	59.87	57.71	88	7.4	179	0.35	39.2	900.8
Hemisphere S.	58.27	61.14	84	7.4	178	0.36	40.4	955.1

5. Conclusions

This project investigates a flexible solar panel for energy on curved surfaces. We employed the actual capability of flexible solar energy conversion in this study, which was conducted utilizing environmental evaluation and environmental techniques centered on pilot projects. Annual energy production on the flat surface was 810 kWh, cylindrical surface 960 kWh, and hemisphere surface 1000 kWh. This shows that the findings were valid concerning RSM analysis. The system output current was limited to 0.36 amps when deployed on the hemispherical surface. Using Taguchi methods, research revealed that the influence of power production factors was surface temperature, irradiation, ambient temperature, wind, and humidity. The economic results indicate that NPV at Flat surface is \$ 697.52, with an IRR of 34.81% and a capital return term of 8.58 years. Cylindrical surfaces and hemispheres each see an increase of \$ 955.18. The investment yield returned 39.29% for cylindrical structures and 40.47% for spherical structures. Consequently, the order of economy in the systems would also be connected to a compact solar system installed on hemispheric, cylindrical and flat surfaces. The following can be stated as a general conclusion. In order to minimize the temperature decrease, the device must be mounted in place of the wind blinds. Radiation and temperature levels are higher than normal. A sensitivity analysis was performed to verify the economic analysis. The Pareto analysis introduces variables that affect system performance, but it is recommended to conduct on-site analysis of similar systems and compare the results during seasonal periods. It is proposed that modular systems be used in flags, towers, conventional structures, biogas tanks, grain storage silos, etc. It is preferable to install electrical systems on one side of the building, which is the largest average of shade. It is recommended that compact structures be used in regions similar to the equator and desert zones.

Nomenclatures

Symbols

A	Area (m ²)
C_{cf}	Net Annual Cash Flow (\$)
CF_i	Cash Flow in the Time Period (\$)
C_{inv}	Initial Investment (\$)
F	Flexibility (Degree)
FF	Fill Factor (%)
FiT	Feed in Tariff (\$.kWh ⁻¹)
G	Irradiance (W.m ⁻²)
I	Current (A)
IRR	Internal Rate of Return (%)
NCF_i	Net Cash Flow for Period i (\$)
NPV	Net Present Value (\$)
P	Power (W)
r	Discount Rate (%)
S_i	Array Layer (m ²)
S/N	Signal to Noise (dB)
T	Temperature (°C)
t	Time (s)

V

Voltage (V)

Greek Symbols

γ Wind Speed (m.s⁻¹)

η Efficiency (%)

Subscript

mmp Maximum Power Point

sc Short Circuit Current

oc Open Circuit Voltage

Abbreviations

a-Si Amorphous Silicon

BCR Benefit Cost Ratio

BIPV Built Integrated Photovoltaic

BOS Balance of System

c-Si Crystalline Silicon

FPVS Flexible Photovoltaic Systems

GHG Greenhouse Gases

PBP Payback Period

PV Photovoltaic

RSM Response Surface Methodology

SNR Signal to Noise Ratio

STC Standard Test Conditions

References

- Abdolbaqi, M. K., Azmi, W. H., Mamat, R., Mohamed, N. M. Z. N., & Najafi, G. (2016). Experimental investigation of turbulent heat transfer by counter and co-swirling flow in a flat tube fitted with twin twisted tapes. *International Communications in Heat and Mass Transfer*, *C(75)*, 295–302. doi: 10.1016/J.ICHEATMASSTRANSFER.2016.04.021
- Al-Falahi, M. D. A., Jayasinghe, S. D. G., & Enshaei, H. (2019). Hybrid algorithm for optimal operation of hybrid energy systems in electric ferries. *Energy*, *187*, 115923. doi: 10.1016/J.ENERGY.2019.115923
- Awad, O. I., Ali, O. M., Mamat, R., Abdullah, A. A., Najafi, G., Kamarulzaman, M. K., Yusri, I. M., & Noor, M. M. (2017). Using fusel oil as a blend in gasoline to improve SI engine efficiencies: A comprehensive review. *Renewable and Sustainable Energy Reviews*, *69*, 1232–1242. doi: 10.1016/J.RSER.2016.11.244
- Azadbakht, M., Shayan, M. E., Jafari, H., Ghajarjazi, E., & Kiapei, A. (2015). Factor Resistance Comparison of a Long Shaft in 955 and 1055 John Deere Grain Combine. doi: 10.5281/ZENODO.1100909
- Azadbakht, M., Esmaeilzadeh, E., & Esmaeili-Shayan, M. (2015). Energy consumption during impact cutting of canola stalk as a function of moisture content and cutting height. *Journal of the Saudi Society of Agricultural Sciences*, *14(2)*, 147–152. doi: 10.1016/j.jssas.2013.10.002
- Azadbakht, M., Shayan, M. E., & Jafari, H. (2013). Investigation of Long Shaft Failure in John Deere 955 Grain Combine Harvester under Static Load. *Universal Journal of Agricultural Research*, *1(3)*, 70–73. doi: 10.13189/UJAR.2013.010305
- Bloem, J. J. J., Lodi, C., Cipriano, J., & Chemisana, D. (2012). An outdoor Test Reference Environment for double skin applications of Building Integrated PhotoVoltaic Systems. *Energy and Buildings*, *50*, 63–73. doi: 10.1016/j.enbuild.2012.03.023
- Braitto, M., Flint, C., Muhar, A., Penker, M., & Vogel, S. (2017). Individual and collective socio-psychological patterns of photovoltaic investment under diverging policy regimes of

- Austria and Italy. *Energy Policy*, 109, 141–153. doi: 10.1016/J.ENPOL.2017.06.033
- Briguglio, M., & Formosa, G. (2017). When households go solar: Determinants of uptake of a Photovoltaic Scheme and policy insights. *Energy Policy*, 108, 154–162. doi: 10.1016/J.ENPOL.2017.05.039
- Chen, J., E, J., Kang, S., Zhao, X., Zhu, H., Deng, Y., Peng, Q., & Zhang, Z. (2019). Modeling and characterization of the mass transfer and thermal mechanics of the power lithium manganate battery under charging process. *Energy*, 187, 115924. doi: 10.1016/J.ENERGY.2019.115924
- Dehghan, M., Rahgozar, S., Pourrajabian, A., Aminy, M., & Halek, F. S. (2021). Techno-economic perspectives of the temperature management of photovoltaic (PV) power plants: A case-study in Iran. *Sustainable Energy Technologies and Assessments*, 45, 101133. doi: 10.1016/j.seta.2021.101133
- Esmaili Shayan, M. (2020). Solar Energy and Its Purpose in Net-Zero Energy Building. In A. Pérez-Fargallo & I. Oropeza-Perez (Eds.), *Zero-energy Buildings. New approaches and technologies*. IntechOpen. doi: 10.5772/intechopen.93500
- Esmaili Shayan, M., Esmaili Shayan, S., & Nazari, A. (2021). Possibility of supplying energy to border villages by solar energy sources. *Energy Equipment and Systems*, 9(3), 279–289. doi: 10.22059/EES.2021.246079
- Esmaili Shayan, M., & Ghasemzadeh, F. (2020). Nuclear Power Plant or Solar Power Plant. In N. Awwad (Ed.), *Nuclear Power Plants - The Processes from the Cradle to the Grave*. London: IntechOpen. doi: 10.5772/intechopen.92547
- Esmaili Shayan, M., & Hojati, J. (2021). Floating Solar Power Plants: A Way to Improve Environmental and Operational Flexibility. *Iranian (Iranica) Journal of Energy & Environment*, 0. Retrieved from http://www.ijee.net/article_140620.html
- Esmaili shayan, M., Najafi, G., & Gorjian, S. (2020). Design Principles and Applications of Solar Power Systems (In Persian) (First Edit). Tehran: ACECR Publication-Amirkabir University of Technology Branch.
- Esmaili Shayan, M., Najafi, G., & Lorenzini, G. (2022). Phase change material mixed with chloride salt graphite foam infiltration for latent heat storage applications at higher temperatures and pressures. *International Journal of Energy and Environmental Engineering* 2021, 1–11. doi: 10.1007/S40095-021-00462-5
- Esmaili Shayan, M., Najafi, G., & Nazari, A. (2021). The Biomass Supply Chain Network Auto-Regressive Moving Average Algorithm. *International Journal of Smart Grid - IjSmartGrid*, 5(1), 15–22. Retrieved from <https://www.ijsmartgrid.ijrer.org/index.php/ijsmartgridnew/article/download/153/pdf>
- Ettefaghi, E., Ghobadian, B., Rashidi, A., Najafi, G., Khoshtaghaza, M. H., Rashchi, M., & Sadeghian, S. (2018). A novel bio-nano emulsion fuel based on biodegradable nanoparticles to improve diesel engines performance and reduce exhaust emissions. *Renewable Energy*, 125, 64–72. doi: 10.1016/j.renene.2018.01.086
- Ghasemzadeh, F., Esmailzadeh, M., & Esmaili shayan, M. (2020). Photovoltaic Temperature Challenges and Bismuthene Monolayer Properties. *International Journal of Smart Grid*, 4(4), 190–195. Retrieved from <https://www.ijsmartgrid.org/index.php/ijsmartgridnew/article/view/131/pdf>
- Ghritlahre, H. K., & Prasad, R. K. (2018). Application of ANN technique to predict the performance of solar collector systems - A review. *Renewable and Sustainable Energy Reviews*, 84(December 2017), 75–88. doi: 10.1016/j.rser.2018.01.001
- Hasanien, H. M. (2018). Performance improvement of photovoltaic power systems using an optimal control strategy based on whale optimization algorithm. *Electric Power Systems Research*, 157, 168–176. doi: 10.1016/j.epsr.2017.12.019
- IEA. (2021). *Global Energy Review 2021 – Analysis* - IEA. Retrieved from <https://www.iea.org/reports/global-energy-review-2021>
- Jäger-Waldau, A. (2021). Overview of the Global PV Industry. Reference Module in Earth Systems and Environmental Sciences. doi: 10.1016/B978-0-12-819727-1.00054-6
- Padmanathan K., Govindarajan, U., Vigna K., Selvi T, S., Jeevarathinam, B. (2018). Integrating solar photovoltaic conversion systems into industrial and commercial electrical energy utilization—A survey. *Journal of Industrial Information Integration*. doi: 10.1016/j.jii.2018.01.003
- Keshtegar, B., Mert, C., & Kisi, O. (2018). Comparison of four heuristic regression techniques in solar radiation modeling: Kriging method vs RSM, MARS and M5 model tree. *Renewable and Sustainable Energy Reviews*, 81(July 2017), 330–341. doi: 10.1016/j.rser.2017.07.054
- Leonard, M. D., & Michaelides, E. E. (2018). Grid-independent residential buildings with renewable energy sources. *Energy*, 148, 448–460. doi: 10.1016/J.ENERGY.2018.01.168
- Liobikienė, G., & Butkus, M. (2021). Determinants of greenhouse gas emissions: A new multiplicative approach analysing the impact of energy efficiency, renewable energy, and sector mix. *Journal of Cleaner Production*, 309, 127233. doi: 10.1016/J.JCLEPRO.2021.127233
- Mat Yasin, M. H., Mamat, R., Najafi, G., Ali, O. M., Yusop, A. F., & Ali, M. H. (2017). Potentials of palm oil as new feedstock oil for a global alternative fuel: A review. *Renewable and Sustainable Energy Reviews*, 79, 1034–1049. doi: 10.1016/J.RSER.2017.05.186
- Mohammadi, M., Ghasempour, R., Razi Astaraei, F., Ahmadi, E., Aligholian, A., & Toopshekan, A. (2018). Optimal planning of renewable energy resource for a residential house considering economic and reliability criteria. *International Journal of Electrical Power & Energy Systems*, 96, 261–273. doi: 10.1016/J.IJEPES.2017.10.017
- Muhammad-Sukki, F., Ramirez-Iniguez, R., Abu-Bakar, S. H., McMeekin, S. G., & Stewart, B. G. (2011). An evaluation of the installation of solar photovoltaic in residential houses in Malaysia: Past, present, and future. *Energy Policy*, 39(12), 7975–7987. doi: 10.1016/J.ENPOL.2011.09.052
- Najafi, G., & Ghobadian, B. (2011). LLK1694-wind energy resources and development in Iran. *Renewable and Sustainable Energy Reviews*, 15(6), 2719–2728. doi: 10.1016/J.RSER.2011.03.002
- Najafi, G., Ghobadian, B., Yusaf, T., & Rahimi, H. (2007). Combustion analysis of a CI engine performance using waste cooking biodiesel fuel with an artificial neural network aid. *American Journal of Applied Sciences*, 756–764.
- O'Shaughnessy, E., Cruce, J., & Xu, K. (2021). Rethinking solar PV contracts in a world of increasing curtailment risk. *Energy Economics*, 98, 105264. doi: 10.1016/J.ENERCO.2021.105264
- Rabab Mudakkar, S., Zaman, K., Shakir, H., Arif, M., Naseem, I., & Naz, L. (2013). Determinants of energy consumption function in SAARC countries: Balancing the odds. *Renewable and Sustainable Energy Reviews*, 28, 566–574. doi: 10.1016/J.RSER.2013.08.006
- Salehi-Isfahani, D., & Mostafavi-Dehzoeei, M. H. (2018). Cash transfers and labor supply: Evidence from a large-scale program in Iran. *Journal of Development Economics*, 135, 349–367. doi: 10.1016/J.JDEVECO.2018.08.005
- Shukla, A. K., Sudhakar, K., Baredar, P., & Mamat, R. (2018). BIPV based sustainable building in South Asian countries. *Solar Energy*, 170, 1162–1170. doi: 10.1016/j.solener.2018.06.026
- Skordoulis, M., Ntanos, S., & Arabatzis, G. (2020). Socioeconomic evaluation of green energy investments: Analyzing citizens' willingness to invest in photovoltaics in Greece. *International Journal of Energy Sector Management*, 14(5), 871–890. doi: 10.1108/IJESM-12-2019-0015/FULL/XML
- Solangi, H., Islam, M.R., Saidur, R., Rahim, N.A., Fayaz, H. (2011). A review on global solar energy policy, *Renewable and Sustainable Energy Reviews*. doi: 10.1016/j.rser.2011.01.007
- Tsantopoulos, G., Arabatzis, G., & Tampakis, S. (2014). Public attitudes towards photovoltaic developments: Case study from Greece. *Energy Policy*, 71, 94–106. doi: 10.1016/J.ENPOL.2014.03.025

Yan, J., Luo, G., Xiao, B., Wu, H., He, Z., & Cao, Y. (2015). Origin of high fill factor in polymer solar cells from semiconducting polymer with moderate charge carrier mobility. *Organic Electronics*, 24, 125–130. doi: 10.1016/J.ORGEL.2015.05.034

Yin, Y., Liu, T., & He, C. (2019). Day-ahead stochastic coordinated scheduling for thermal-hydro-wind-photovoltaic systems. *Energy*, 187, 115944. doi: 10.1016/J.ENERGY.2019.115944

Zeb, R., Salar, L., Awan, U., Zaman, K., & Shahbaz, M. (2014). Causal links between renewable energy, environmental degradation and economic growth in selected SAARC countries: Progress towards green economy. *Renewable Energy*, 71, 123–132. doi: 10.1016/J.RENENE.2014.05.012.



© 2022. The Authors. This article is an open access article distributed under the terms and conditions of the Creative Commons Attribution-ShareAlike 4.0 (CC BY-SA) International License (<http://creativecommons.org/licenses/by-sa/4.0/>)